Bioorganic & Medicinal Chemistry 21 (2013) 653–659

Contents lists available at SciVerse ScienceDirect

Bioorganic & Medicinal Chemistry

journal homepage: www.elsevier.com/locate/bmc

Molecular recognition of indole derivatives by polymers imprinted with indole-3-acetic acid: A QSPR study

Ivana Porobić [a], Darko Kontrec [b], Milan Šoškić [a,*]

[a] Department of Chemistry, Faculty of Agriculture, University of Zagreb, Svetošimunska 25, 10000 Zagreb, Croatia
[b] Department of Organic Chemistry and Biochemistry, Ruđer Bošković Institute, Bijenička 54, 10000 Zagreb, Croatia

ARTICLE INFO

Article history:
Received 5 August 2012
Revised 19 November 2012
Accepted 29 November 2012
Available online 8 December 2012

Keywords:
Indole derivatives
Molecularly imprinted polymers
High-performance liquid chromatography
Retention factors
Quantitative structure–property relationships

ABSTRACT

Three molecularly imprinted polymers (MIPs) were prepared using the phytohormone indole-3-acetic acid (IAA) as a template molecule, 4-vinylpyridine (MIP-1 and MIP-2) or *N*,*N*-dimethylaminoethyl methacrylate (MIP-3) as functional monomers, ethylenglycol dimethacrylate as a cross linker and acetonitrile (MIP-1), a methanol–water mixture (MIP-2) or chloroform (MIP-3) as porogens. Retention factors for IAA and 29 indole derivatives were determined by high-performance liquid chromatography, using the molecularly imprinted polymers as stationary phases and acetonitrile as an eluent. High correlations between selectivity factors of above mentioned polymers indicate that their retention mechanisms are basically the same. A quantitative structure–property relationships analysis revealed that the presence of the terminal carboxyl group on the 3-side chain plays an essential role in the binding of the indole derivatives to the polymers. The derivatives without the carboxyl group exhibit a drastically lower affinity toward the polymers. Another factor which favors the binding is electronic density of indole nucleus. Substituents with electro-withdrawing properties enhance the binding, while electro-donating substituents have the opposite effect. The length of the 3-side chain also affects the binding. Indole-3-carboxylic acid having the carboxyl group directly attached to the ring as well as the derivatives whose side chain is longer than that of IAA bind to the polymers with a lower affinity.

1. Introduction

Molecular recognition plays an important role in many biological processes. The studies of molecular recognition in model systems, which mimic the biological receptors, are important for understanding the recognition phenomena observed in nature, in particular if natural receptors are not available.

Molecular imprinting[1] is a technique which makes possible creation of synthetic polymer receptors with the enhanced selectivity for a target (template) molecule. The method is based on copolymerization of a functional polymer and a cross-linker in the presence of the template molecule. After removal of the template, specific recognition places remain in the rigid polymer matrix, which are by size, shape and arrangement of functional groups complementary to the template. Molecularly imprinted polymers (MIPs) have found application in many areas of chemistry and biology including chromatographic separations,[2] biosensors[3] and artificial antibodies[4] and receptors.[5]

Indole-3-acetic acid is the principle natural auxin which regulates practically all aspects of plant growth and development.[6] A number of proteins are able to bind IAA,[7] but recent studies[8,9] identified 'transport inhibitor response 1 protein' (TIR1) as the long term sought auxin receptor. Crystallographic analysis[10] revealed that the carboxyl group of IAA interacts with polar amino acid residues within the auxin-binding pocket of TIR1, while the indole ring is in contacts with hydrophobic residues, including the aromatic rings of phenylalanine (Phe) 79 and 82. 'Auxin binding protein 1' (ABP1)[11] also attracted much attention as a putative receptor for IAA, but its physiological role is not yet clear.

Low concentration of IAA in plant tissue and presence of interfering substance makes its isolation difficult and time consuming. In an effort to develop selective sorbents, which will speed up isolation of auxins from plant extracts, several molecular imprinted polymers specific for IAA[12–15] were synthesized and characterized, but their selectivity to indole derivatives was tested on a limited number of structural analogs.

Here we report the preparation and characterization of two novel synthetic polymers specific for IAA and its close structural analogues. In order to learn more about the molecular recognition properties of the obtained polymers, we performed a QSPR analysis correlating the retention factors of IAA and 29 indole derivatives with a series of physico-chemical and structural descriptors.

* Corresponding author. Tel.: +385 (0) 1 2393 872; fax: +385 (0) 1 2315 300.
E-mail address: msoskic@agr.hr (M. Šoškić).

0968-0896/$ - see front matter © 2012 Elsevier Ltd. All rights reserved.
http://dx.doi.org/10.1016/j.bmc.2012.11.048

2. Results and discussion

2.1. Synthesis and characterization of the polymers

Two novel synthetic polymers (poly-4-vinylpyridine-co-ethyleneglycol dimethacrylates) specific for IAA and its close structural analogues (Fig. 1) were synthesized, using acetonitrile (MIP-1) or a methanol-water mixture (MIP-2) as porogens. For comparison, poly-*N*,*N*-dimethylaminoethyl methacrylate-co-ethyleneglycol dimethacrylate (MIP-3), whose synthesis had been reported recently,[13] was also prepared. Corresponding reference non-imprinted polymers (NIPs) were prepared in the same way as the molecularly imprinted polymers but without addition of the target molecule.

2.1.1. Spectroscopic and morphological characterization of the polymers

The chemical and morphological characterization of the novel molecularly imprinted (MIP-1 and MIP-2) and corresponding reference polymers were performed by Fourier-transform infra-red spectroscopy (FTIR), Brunauer–Emmett–Teller (BET) analysis and scanning electron microscopy (SEM).

The spectroscopic analysis has shown that the spectra of all four polymers are very similar, with characteristic and most intensive bands at 1730 ± 3 and 1157 ± 2 cm^{-1}, assigned to C=O and C–O stretching, respectively. Similarity of the spectra (Fig. 2, spectra of MIP-2 and NIP-2 are not shown) indicates that neither presence of the template, nor the porogens used in the preparation of the polymers, affected the chemical composition of the synthesized polymers. However, the porogens markedly affected the morphology of the obtained polymers, which is clearly seen from the significant differences in their specific surface areas (Table 1) and corresponding SEM images (Fig. 3).

2.1.2. Chromatographic evaluation

The selectivity of the molecularly imprinted polymers for a series of indolic compounds were explored by high-pressure liquid chromatography, using the imprinted and non-imprinted polymers as stationary phases and acetonitrile as an eluent.

When an analyte passes through the column packed with a molecularly imprinted polymer it interacts with both specific and nonspecific binding sites. On the other hand, the binding of the analyte to the non-imprinted polymer is mainly nonspecific in nature. Hence, the retention observed on the corresponding non-imprinted polymer is commonly used as a measure for the nonspecific bindings of the analyte. It should be pointed out, however, that this is strictly valid only when a MIP and a NIP are morphologically identical.

It can be seen from Table 2 that IAA is considerably more retained on MIPs than on the corresponding reference polymers, which confirms the presence of the specific recognition sites on the synthesized MIPs. It can also be seen that the retention factor of the target molecule is significantly higher for MIP-3 than for MIP-1 and MIP-2. It is not unexpected result since amino group of *N*,*N*-dimethylaminoethyl methacrylate can form stronger hydrogen (partial ionic) bonds with the acidic carboxyl group of IAA, than nitrogen atom of 4-vinylpyridine. The difference in retention factors of MIP-1 and MIP-2 for IAA can be explained[16] by so called 'solvent memory effect'. It was found that the optimal eluent for rebinding of the target molecule is generally the solvent used in the preparation of the molecularly imprinted polymer. It appears that the imprinted binding sites 'memorize' the structure of the (partially) solvated target molecule. Since non-imprinted polymers do not contain the imprinted binding sites, it seems that the differences in the retention factors of NIP-1 and NIP-2 can be attributed to the differences in their morphology. The influence of porogens on the polymer morphology is well documented in literature.[17]

Comparison of imprinting factors shows that the nonspecific bindings play significant role on MIP-3 whereas they are practically negligible in case of MIP-2. High proportion of nonspecific interactions on the MIP-3 suggests that a great number of monomers are not incorporated in the specific binding sites, but that they are scattered in the polymer matrix as a result of higher molar ratio between the functional monomer and the target molecule used in the synthesis of this polymer, relative to the 4-vinylpiridine polymers. For the rest of indolic compounds the imprinting factors (data not shown) range from 1.1 to 1.5 for MIP-3, from 1.7 to 3.3 for MIP-1 and from 7.3 to 23.7 for MIP-2.

The selectivity factors (α) for the synthesized polymers are displayed in Table 3, along with the retention factors for MIP-1 and NIP-1. It can be concluded from high correlations among the selectivity factors (r^2 >0.9) that all the three polymers follow very similar selectivity pattern. Generally, they recognize well the indole-3-carboxylic acids, while their recognition ability for the indolic compounds without carboxyl group at substitution position three is poor. Furthermore, the selectivity factors for several halogen derivatives of IAA exceed one, indicating that these compounds bind more strongly to the polymers than the target molecule used in the imprinting process. In other words, the prepared polymers are group specific: they selectively recognize not only the target molecule but also its structurally close analogues.

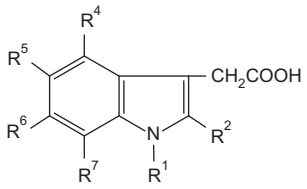

Figure 1. General structure of indole derivatives.

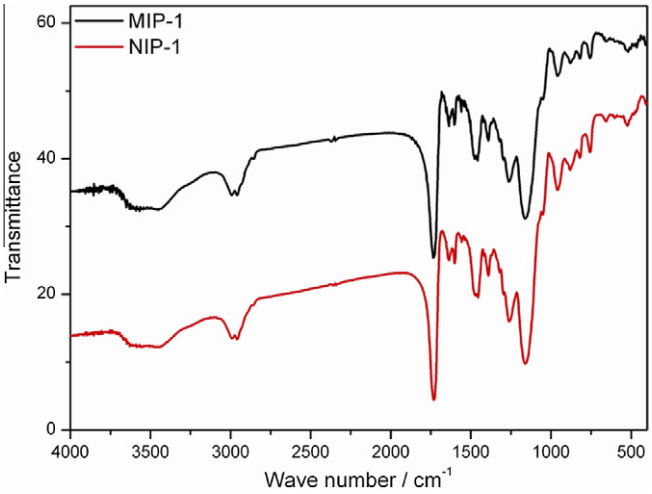

Figure 2. FTIR spectra of imprinted (MIP-1) and nonimprinted (NIP-1) polymer.

Table 1
Specific surface area of synthesized polymers

Polymer	Specific surface area (m^2/g)
MIP-1	401.3
NIP-1	336.7
MIP-2	60.9
NIP-2	96.5

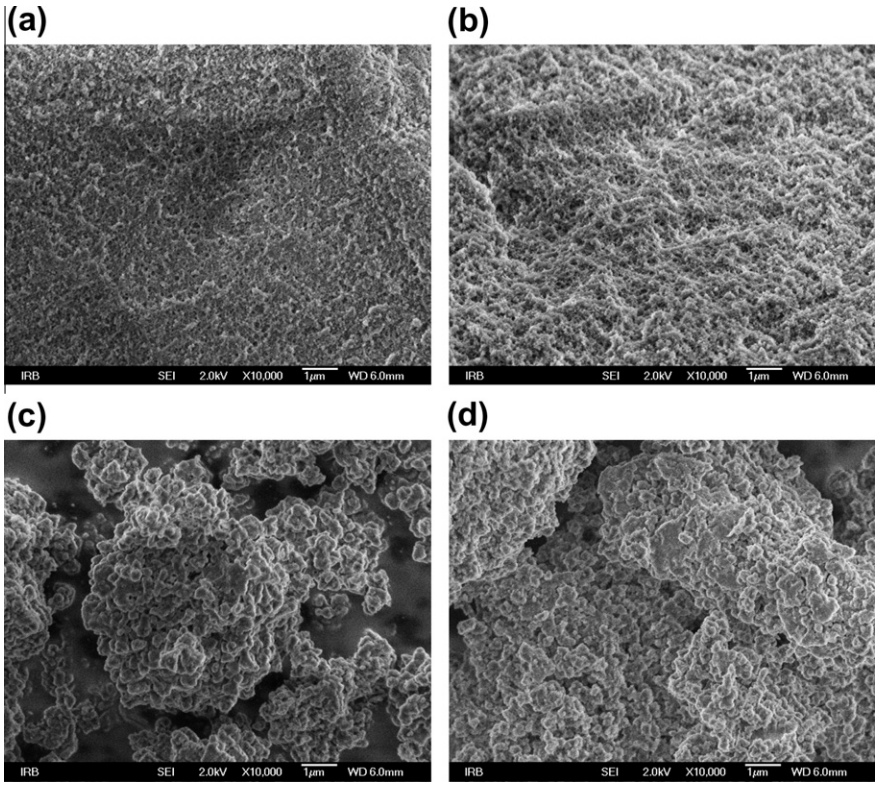

Figure 3. SEM images of (a) MIP-1, (b) NIP-1, (c) MIP-2 and (d) NIP-2.

Table 2
Retention (k) and imprinting factors (IF) for the template molecule (IAA) determined on different MIP and NIP columns (details given in the text)

Polymer	k	IF
MIP-1	4.72	3.3
NIP-1	1.44	
MIP-2	3.77	14.0
NIP-2	0.27	
MIP-3	19.52	1.4
NIP-3	14.00	

Table 3
Retention (k) and selectivity factors (α) for 30 indole derivatives determined on the three different molecularly imprinted polymers

No.	Compound	k_{MIP-1}	k_{NIP-1}	α_{MIP-1}	α_{MIP-2}	α_{MIP-3}
1.	IAA	4.72	1.44	1	1	1
2.	Indole-3-carboxylic acid	3.49	1.60	0.74	–	–
3.	Indole-3-propionic acid	3.29	1.48	0.70	0.94	0.83
4.	Indole-3-butyric acid	2.96	1.39	0.63	0.81	0.71
5.	Indole-3-acrylic acid	3.68	1.66	0.78	–	–
6.	1-Me-IAA	2.20	0.93	0.47	0.64	0.67
7.	2-Me, 5-OMe-IAA	2.39	0.96	0.51	0.58	0.68
8.	4-F-IAA	4.27	1.32	0.90	0.89	–
9.	4-Cl-IAA	4.26	1.45	0.90	0.88	1.14
10.	5-F-IAA	4.71	1.48	1.00	0.89	1.14
11.	5-Cl-IAA	5.90	1.87	1.25	1.26	1.50
12.	5-Br-IAA	6.38	2.08	1.35	1.43	1.65
13.	5-Me-IAA	3.76	1.28	0.80	0.87	–
14.	5-OMe-IAA	3.20	1.16	0.68	0.73	0.88
15.	5-OBz-IAA	3.72	1.35	0.79	0.94	–
16.	5,7-Cl_2-IAA	7.24	2.70	1.53	1.95	–
17.	6-F-IAA	4.52	1.47	0.96	1.05	–
18.	6-Cl-IAA	6.01	1.99	1.27	1.37	–
19.	6-Me-IAA	4.32	1.34	0.92	0.92	–
20.	7-F-IAA	5.84	1.75	1.24	1.33	–
21.	7-Cl-IAA	6.25	2.08	1.32	1.53	–
22.	7-Br-IAA	7.18	2.32	1.52	1.67	–
23.	7-Me-IAA	3.89	1.29	0.82	0.91	–
24.	Me-ester-IAA	0.26	0.15	0.06	0.04	0.02
25.	Et-ester-IAA	0.22	0.13	0.05	0.06	0.02
26.	Indole-3-acetamide	0.54	0.24	0.11	0.11	0.03
27.	Indole-3-ethanol	0.58	0.30	0.12	0.12	0.04
28.	Indole-3-methyl ketone	0.38	0.21	0.08	–	–
29.	Indole-3-acetonitrile	0.22	0.14	0.05	–	–
30.	Indole-3-ol-acetate ester	0.25	0.15	0.05	–	–

It should also be mentioned that there exist a high correlation among capacity factors determined on a particular MIP and corresponding NIP column.

2.2. Quantitative structure–property relationships analysis

In an effort to rationalize above mentioned chromatographic observations a QSPR analysis was performed. We present here a model which accurately predicts retention factors (expressed as $\log k$) for the indole derivatives determined on the MIP-1 column. The experimental and calculated retention factors for 30 indole derivatives together with the physico-chemical and structural parameters which appear in the final regression model (Eq. (3)) are given in Table 4. The compounds **1**–**24** were used as a training set while compounds **25**–**30** were used for validation of the derived model. A total of 37 descriptors were screened while developing the model: $\log P$ values, π values and Veerloop's steric constants (L, B_1, B_5) for substituent position 3–7, Hammett's electronic sigma constants (σ_m, σ_p) for substituent positions 4–7, valence zero-order molecular connectivity index ($^0\chi^v$), valence first-order molecularly connectivity index ($^1\chi^v$), valence third-order cluster molecularly connectivity index ($^3\chi^v_c$), valence fourth-order path-cluster molecular connectivity index ($^4\chi^v_{pc}$), number of H-bond donors (*H*d), number of H-bond acceptors (*H*ac), molar volume (MgVol) and indicator variables I_1 and I_2, which meaning will be given later.

Table 4
Sum of Hammett constants, number of hydrogen bond donors and indicator variables (meaning given in the text) plus observed and calculated retention factors of the studied indole derivatives obtained on MIP-1 column

No.	Compound	$[\sigma_p (R^5 + R^6) + \sigma_m (R^7)]$	*H*d	I_1	I_2	$\log k_{MIP\text{-}1}$	
						Exp.	Eq. (3)
1.	IAA	0	2	1	0	0.67	0.66
2.	Indole-3-carboxylic acid	0	2	1	1	0.54	0.52
3.	Indole-3-propionic acid	0	2	1	1	0.52	0.52
4.	Indole-3-butyric acid	0	2	1	1	0.47	0.52
5.	Indole-3-acrylic acid	0	2	1	1	0.57	0.52
6.	1-Me-IAA	0	1	1	0	0.34	0.32
7.	2-Me, 5-OMe-IAA	−0.27	2	1	1	0.38	0.40
8.	4-F-IAA	0	2	1	0	0.63	0.66
9.	5-F-IAA	0.06	2	1	0	0.67	0.69
10.	5-Cl-IAA	0.23	2	1	0	0.77	0.76
11.	5-Br-IAA	0.23	2	1	0	0.80	0.76
12.	5-Me-IAA	−0.17	2	1	0	0.58	0.59
13.	5-OBz-IAA	−0.23	2	1	0	0.57	0.56
14.	6-Cl-IAA	0.23	2	1	0	0.78	0.76
15.	6-Me-IAA	−0.17	2	1	0	0.64	0.59
16.	7-F-IAA	0.34	2	1	0	0.77	0.81
17.	7-Cl-IAA	0.37	2	1	0	0.80	0.82
18.	7-Br-IAA	0.39	2	1	0	0.86	0.83
19.	7-Me-IAA	−0.07	2	1	0	0.59	0.63
20.	Me-ester-IAA	0	1	0	0	−0.58	−0.61
21.	Indole-3-acetamide	0	2	0	0	−0.26	−0.26
22.	Indole-3-ethanol	0	2	0	0	−0.23	−0.26
23.	Indole-3-ol-acetate ester	0	1	0	0	−0.60	−0.61
24.	Indole-3-acetonitrile	0	1	0	0	−0.66	−0.61
25.	4-Cl-IAA	0	2	1	0	0.63	0.66
26.	5-OMe-IAA	−0.27	2	1	0	0.50	0.55
27.	5,7-Cl_2-IAA	0.60	2	1	0	0.86	0.92
28.	6-F-IAA	0.06	2	1	0	0.66	0.69
29.	Et-ester-IAA	0	1	0	0	−0.66	−0.61
30.	Indole-3-methyl ketone	0	1	0	0	−0.42	−0.61

Initially we derived a model (Eq. (1)) for IAA and its ring-substituted derivatives (compounds **1** and **8**–**19**). For their atypical retention behavior, 1-Me-IAA and 2-Me, 5-OMe-IAA were excluded from the analysis at this phase of the model development. Using linear regression analysis a statistically significant one-parameter model was obtained which explains more than 90% variations in retention factors of the indole-3-acetic acids,

$$\log k\ (\mathrm{MIP}_1) = 0.662\ (\pm 0.021) + 0.429\ (\pm 0.091)\ [\sigma_p\ (R^5 + R^6) + \sigma_m\ (R^7)]$$
$$n = 13 \quad r^2 = 0.907 \quad s = 0.031 \quad F^{1,11} = 107.7$$
$$q^2_{LOO} = 0.868 \quad \mathrm{PRESS} = 0.015 \qquad (1)$$

where $[\sigma_p (R^5 + R^6) + \sigma_m (R^7)]$ is sum of Hammett sigma constants of substituents in the positions 5, 6 and 7. In this and the following equations the 95% confidence intervals are given in parentheses. We employ here Hammett's σ_{para} constants for 5- and 6-substituents and σ_{meta} for 4- and 7-substituents, in analogy to an approach used to rationalize substituent effects on the acidity of the indole NH.[18,19] The model suggests that retention factors are significantly influenced by the electron density in the indole nucleus. The positive coefficients of $[\sigma_p (R^5 + R^6) + \sigma_m (R^7)]$ indicate that electron-withdrawing substituents enhance the retention factors of the indole-3-acetic acids, while electron-donating substituents have the opposite effect. As can be seen this effect was not observed for 4-substituted derivatives (4-F-IAA and 4-Cl-IAA). In contrast to the 7-substituted analogues, their retention factors are somewhat lower as compared to IAA (Table 4). It appears that reason for this is not steric hindrance within the binding cavity since these compounds show a similar retention pattern on the NIP column (Table 3).

The model which includes all compounds used in the training set is as follows:

$$\log k\ (\mathrm{MIP}_1) = -0.925\ (\pm 0.147) + 0.542\ (\pm 0.166)\ [\sigma_p\ (R^5 + R^6) + \sigma_m\ (R^7)] + 0.889\ (\pm 0.088)\ I_1 + 0.328\ (\pm 0.095)\ H\mathrm{d}$$
$$n = 24 \quad r^2 = 0.983 \quad s = 0.067 \quad F^{3,20} = 387.3$$
$$q^2_{LOO} = 0.977 \quad \mathrm{PRESS} = 0.122$$

Indicator variable I_1 differentiates indole-3-carboxylic acids ($I_1 = 1$) from the indolic compounds without carboxyl group at the substituent position 3 ($I_1 = 0$). Clearly, the carboxylic group on the 3-side chain is essential for recognition of indolic compounds by the polymer matrix (Fig. 4). Positive regression coefficients of I_1 demonstrates that the retention factors of the indole-3-carboxylic acids, all other factors being equal, are about seven times higher than those of compounds without the carboxyl group. The variable *H*d indicates that, apart from the carboxyl group, the NH group of indole ring as well as the hydrogen bond

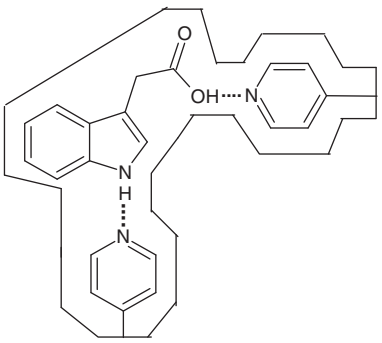

Figure 4. Proposed interactions between the MIP and indole-3-acetic acids.

donor groups on the 3-side chain of indole-3-ethanol and of indole-3-acetamide are also involved in hydrogen bonding with pyridine moiety, reinforcing in that way the binding affinity. It best illustrates a markedly reduced retention time of 1-Me-IAA (Table 4) in which a hydrogen atom of the NH group is replaced by a methyl group. (It should be pointed out that the free NH group is not required for high-affinity binding of the indole-3-carboxylic acids to human serum albumin and 3,5-dinitrobenzoyl-phenylglycine.[20,21]) The analysis of residuals showed that the retention factors of several compounds (i.e. indole-3-carboxylic acid, indole-3-propionic acid, indole-3-butyric acid, indole-3-acrylic acid (compounds **2**–**5**) and 2-Me, 5-OMe-IAA (compound **7**)) were systematically overestimated. It appears that lower retention factors of compounds **2**–**5** are caused by steric misfit of their 3-side chain which connects the carboxyl group with the indole ring. The side chain of compounds **3**–**5** is longer than the acetic acid moiety of the imprinted molecule, whereas the carboxyl group of indole-3-carboxylic acid is directly attached to the indole ring. On the other hand, it appears that methyl group at the position 2 interfere with the accessibility of the carboxyl group and thus prevent the proper orientation of indole-3-acetic acids within the binding cavity. As both the negative steric effects are comparable in the magnitude, they are described by a common indicator variable, I_2. I_2 takes one for compounds **2**–**5** and **7**, otherwise its values amounts 0. Although the three-parameter model accounts for 98% variations in the retention factors, huge decrease in standard deviation (about 49%) and PRESS (approximately 71%) in Eq. (3) justifies introduction of another variable the model:

$$\log k\,(MIP_1) = -0.953\,(\pm 0.075) + 0.435\,(\pm 0.089)\,[\sigma_p\,(R^5 + R^6) + \sigma_m\,(R^7)] + 0.921\,(\pm 0.045)\,I_1 + 0.348\,(\pm 0.049)\,Hd - 0.144\,(\pm 0.039)\,I_2$$
$$n = 24 \quad r^2 = 0.996 \quad s = 0.034 \quad F^{4,19} = 1155.0$$
$$q^2_{LOO} = 0.993 \quad \text{PRESS} = 0.035 \qquad (3)$$

At other substituent positions no clear steric effects were observed. Thus even compound **7** with bulky benzyloxy group at the position 5 seems to fit well into the imprinting cavity, although one can speculate that reason for this is that only the indole-3-acetic acid moiety occupies the cavity while the benzyloxy group protrudes from it. Since the imprinted cavities are clearly large enough to accommodate majority of the indolic compounds, binding affinities of these compounds are mostly determined by the strength of the hydrogen bonds which they make with the polymer matrix and presumably by π–π stackings between the indole ring and pyridine moieties. Hence, it is not surprising that several halogen derivatives of IAA were retained longer on the MIP column than the template molecule. A high correlation between the retention factors obtained on the MIP and NIP columns (r^2 >0.9) can also be explained by the fact that steric fit does not play an important role in binding of these compounds to the imprinting sites. Nevertheless, the distinctively higher retention factors determined on the MIP column demonstrate that the binding interactions of the indolic compounds with randomly distributed pyridine moieties on the NIP column are far less effective than the ones with properly oriented functional groups inside the cavities. It is also important to note that steric constraints for the compounds **2**–**5** were not detected on the NIP column, which confirms our assumption that lower retention factors determined for these compounds on the MIP stationary phase are result of the imprinting effect.

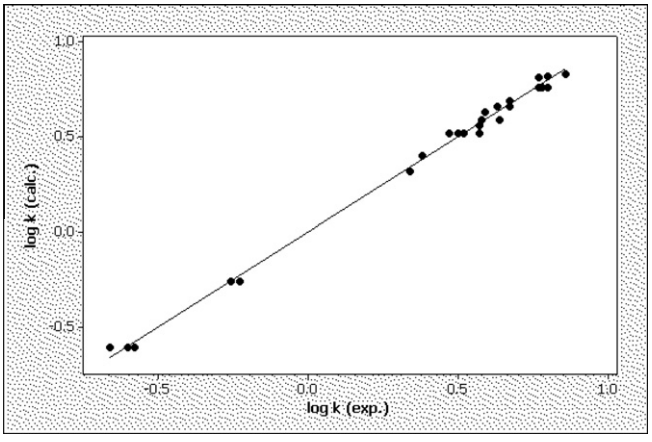

Figure 5. The observed versus calculated log$k$ values for the studied indole derivatives (Eq. (3)).

Table 5
Correlation matrix (r) between predictor variables (Eq. (3))

	$\sigma_p\,(R^5 + R^6) + \sigma_m\,(R^7)$	Hd	I_1	I_2
$\sigma_p\,(R^5 + R^6) + \sigma_m\,(R^7)$	1			
Hd	0.1	1		
I_1	0.12	0.60	1	
I_2	0.28	0.23	0.26	1

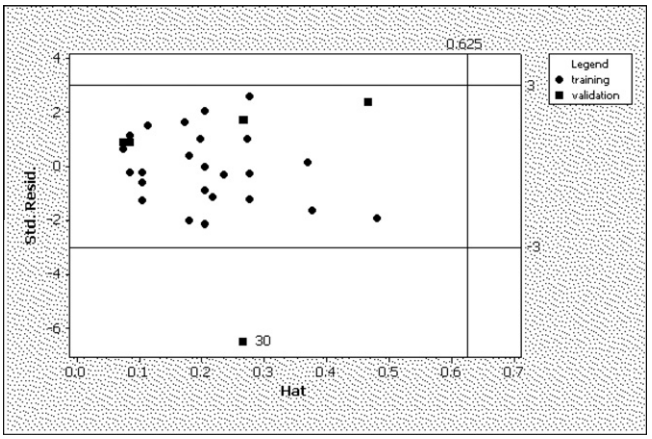

Figure 6. Williams plot of standardized residual versus hat values for the final model (Eq. (3)).

The statistical parameters of Eq. (3) show that model is robust. A plot of the observed retention factors of the indole derivatives versus the log$k$ values calculated by Eq. (3) is given in Figure 5. The pairwise correlations for the descriptor variable appearing in Eq. (3) are displayed in Table 5.

The probability of chance correlation for the final model (Eq. (3)) was tested using the Y-scrambling procedure, which was repeated 300 times. The very low r^2 and q^2_{LOO} values of the models obtained with random responses (data not shown) strongly suggest that the model is not a result of chance correlation.

The quality of the model was further checked by external validation using validation set of six compounds (compounds **25**–**30** in Table 4). The high value of q^2 (0.978) and relatively low value of $SDEP_{EXT}$ (0.088) obtained in this test confirmed the robustness of the model.

The Williams plot (Fig. 6) shows that only log$k$ for compounds **30** from validation set is incorrectly predicted. Its standardized residual in the prediction is higher than the cutoff value of 3σ. Although a response outlier, the compounds belongs to the applicability domain of the model, since its leverage value is lower than the critical one (h^* = 0.625).

Finally, we compared the log$k$ values of the indole-3-acetic acids determined on the MIP-1 with their growth promoting

activities in *Avena* coleoptiles.[19] A direct correlation between our results and growth promoting activities of the indole-3-acetic acids in plants was not found. It worth nothing, however, that similarly as in case of their binding to the polymers, the derivatives of IAA with electro-withdrawing substituents tends to be stronger auxins than the analogues with electro-donating substituents.

3. Conclusion

Three different molecularly imprinted polymers that specifically bind indole-3-acetic acid and their closely related derivatives were prepared and characterized. The polymers based on vinylpyridine as a functional monomer (MIP-1 and MIP-2) exhibit lower affinities to the indole derivatives, but higher imprinting factors as compared to poly-*N*,*N*-dimethylaminoethyl methacrylate co-ethyleneglycol dimethacrylate (MIP-3).

High correlations between selectivity factors of the above mentioned polymers indicate that they share the similar recognition mechanism. QSPR analysis has shown that the presence of the carboxyl group in the 3-side chain is necessary for the strong binding of these compounds to the polymers. The compounds without the carboxyl group have significantly lower retention factors. The lower retention factors of the indole carboxylic acids having the longer or shorter 3-side chain in comparison to the template molecule (indole-3-acetic acid) additionally confirm the importance of the carboxyl group in the process of molecular recognition of these compounds. Electro-withdrawing substituents on the indole ring increase, while electro-donating substituents decrease the binding capacity of the indole derivatives, affecting the strength of hydrogen bonds between the indole NH group and the polymer matrix as well as aromatic interactions between the indole compounds and the vinyl pyridine residues.

4. Experimental

4.1. Chemicals

All chemicals were of analytical grade or better. Acetonitrile of HPLC grade was used as the mobile phases. *N*,*N*-dimethylaminoethyl methacrylate, 4-vinylpyridine, ethylenglycol dimethacrylate (EGDMA) and 2,2′-azobisisobutyronitrile (AIBN) were used as supplied by manufacturer.

4.2. Preparation of polymers

4.2.1. Preparation of the molecularly imprinted polymers with 4-vinylpyridine as functional monomer

The polymers were synthesized using a procedure similar to that proposed for preparation of the molecularly imprinted polymer for 2,4,5-trichlorophenoxyacetic acid:[22] 3.525 mmol IAA (target molecule), 3.525 mmol 4-vinylpyridine (functional monomer), 23.55 mmol EGDMA (cross linker) and 0.449 mmol AIBN (initiator) were dissolved in 5.55 mL of acetonitrile (MIP-1) as porogen. In preparation of MIP-2, a methanol: water mixture (3:1, v/v) was used as porogen instead of acetonitrile. In order to remove dissolved molecular oxygen the pre-polymerization mixture was sparged with nitrogen gas for 5 min and than left to polymerize over night at 65 °C in a water bath (thermal initiation). The obtained bulk polymer was crushed and mechanically ground by mixer mill MM 200 (Retsch, GmbH & Co KG, Germany). The target molecule was removed from the polymer matrix by repeated Soxlet extractions with a methanol: acetic acid mixture (9:1, v/v). The polymer was than wet sieved on the analytical sieve shaker AS 200 basic ((Retsch, GmbH & Co KG, Germany) to yield a particle size of 25–45 μm. The remaining fine particles (<5 μm) were removed by repeated sedimentation in acetone. Finally, the 25–45 μm range size particles were oven dried overnight at 60 °C and stored at ambient temperature.

4.2.2. Preparation of the molecularly imprinted polymers with *N*,*N*-dimethylaminoethyl methacrylate as functional monomer

The polymer was prepared according to previously described procedure[13] with minor modifications. IAA (1.5 mmol), *N*,*N*-dimethylaminoethyl methacrylate (6 mmol), EGDMA (30 mmol) and AIBN (19 mmol) were dissolved in 74 mmol of chloroform, stabilized by amylene, as porogen. After degassing, the reaction mixture was irradiated with UV light (264 nm) for 17 h at 4 °C. This was followed by heating at 80 °C for 3 h. The polymer was ground and sieved to yield a particle size of 5–25 μm.

The non-imprinted polymers were prepared in the same way as corresponding molecularly imprinted polymers but without addition of the target molecule.

4.3. Column packing

The polymers were slurry packed into 150 × 4.6 mm i.d. stainless steel HPLC columns using a Knauer pneumatic HPLC pump (Knauer, Berlin, Germany). The particles were slurred in an ethanol: water mixture (1:1, v/v) and packed into HPLC columns at a maximum pressure of 200 bar, using a compressed gas driven slurry packer and methanol as pushing liquid.

4.4. Liquid chromatography

4.4.1. HPLC instruments

The selectivity of poly-*N*,*N*-dimethylaminoethyl methacrylate-co-ethyleneglycol dimethacrylate was determined on Shimadzu Scientific Instruments (Shimadzu Corporation, Kyoto, Japan). The instrument is composed of Prominence degasser DGU-20 A5, Prominence Liquid Chromatograph LC-20 AT and Prominence UV/VIS Detector Shimadzu. Chromatographic data were processed before printing by computer program Shimadzu EZStart Version 7.3 Sp1 Build 13 (Shimadzu Scientific Instruments, Shimadzu Corporation, Kyoto, Japan).

The selectivity of poly-4-vinylpyridine-co-ethyleneglycol dimethacrylates were determined on Varian 920-LC (Agilent Technologies, Santa Clara, CA, United States) equipped with a low pressure quaternary pump with built in four channel Degasser™, a photodiode array detector, a column heater and an auto sampler with 100 μL sample loop. The system is controlled by Varian Galaxie™ Chromatography Software.

4.4.2. Determination of retention factors

Acetonitrile was used as mobile phase for both the columns filled with poly-4-vinylpyridine-co-ethyleneglycol dimethacrylate and a column filled with poly-*N*,*N*-dimethylaminoethyl metacrylate-co-ethyleneglycol dimethacrylate. Retention times (t_r) of indolic compounds were determined independently, injecting 20 μL of the stock solution (1 mg/mL). Flow rate was 1.0 mL/min. The analysis were carried out at 28 °C. The retention time was average of at least two measurements. The average error for retention times was about 2%. The dead time (t_0) was determined from the retention time of acetone which is not retained by the column. The chromatographic retention of the solutes was expressed as the retention factor (k):

$$k = (t_r - t_0)/t_0 \quad (4)$$

The selectivity factor (α) was calculated as:

$$\alpha = k_{ind}/k_t \quad (5)$$

where k_{ind} is retention factor of an indolic compound and k_t is retention factor of the template molecule (IAA).

Imprinting factor (IF) was calculated as:

$$IF = k_{ind}\ (MIP)/k_{ind}(NIP) \quad (6)$$

where k_{ind} (MIP) is retention factor of an indolic compound on a MIP column and k_{ind} (NIP) is retention factor of the compound on a NIP column.

4.5. FTIR spectroscopy

FTIR spectra of all samples were measured on ABB Bomem MB102 spectrometer, equipped with CsI and DTGS detector, in transmission mode with the nominal resolution of 4 cm^{-1} and 10 scans. The samples were measured as pellets in KBr matrices.

4.6. Specific surface area

Specific surface areas of the polymers were determined by BET analysis carried out on Flowsorb II 2300 (Micrometrics, GA, USA).

4.7. Scanning electron microscopy

Scanning electron micrographs were taken on a thermal field emission scanning electron microscope; model JSM-7000F, manufactured by JEOL LTD.

4.8. Data analysis

4.8.1. Molecular descriptors

The molecular descriptors used in this study were either taken from a standard compilation[23] or were calculated by the commercial softwares TSAR 3.3 for Windows[24] and Bio-Loom for Windows.[25]

4.8.2. Model generation and validation

The data set was randomly divided into a training set (80% compounds of the whole data set) and a validation set (20% compounds of the whole data set) using a training/validation set splitting routine available in MobyDigs software.[26] The training set was used for generation of the QSPR models. The most appropriate descriptors for the QSPR modeling were selected by the stepwise multiple linear regression technique[27] as implemented in TSAR 3.3. In the stepwise regression the first descriptor which enters the model is one with the highest correlation coefficient with response variable. New descriptors are then added one at a time and their importance for the model is checked by *F*-statistics. If the *F* value of a descriptor falls bellow a prespecified value the variable is removed. At each step, before a new variable is added, it is checked if the descriptors already included in the model can be removed. The procedure terminates when no more variables can be added or removed from the model according to the prespecified *F*-to-enter and *F*-to-remove values. In our case *F*-to-enter and *F*-to-remove values were set to four.

In all regression equations n is the number of compounds used in the analysis, r^2 is the squared correlation coefficients, s is the standard deviation of the estimates, and F is the ratio of the variance accounted for regression and the residual variance. The degrees of freedom (k, n-k-1) associated with F are specified in the superscript, wherein k is the number of independent variables in the equation.

The robustness and predictive ability of the models were evaluated by internal and external validation techniques[28–30] using MobyDigs software. The models were internally validated by leave-one-out and response randomization (Y-scrambling) procedure. The validation parameters considered in the leave-one-out procedure were q^2_{LOO} (the sum of squared prediction errors from the leave-one-out cross-validation analysis) and PRESS (the sum of squared prediction errors from the leave-one-out cross-validation analysis).

In the response randomization procedure, the Y data of the original model are randomized and a new regression model is generated using intact X data. The procedure is usually repeated several hundred times. If the r^2 and q^2_{LOO} values of the thus obtained models are, in general, significantly lower then those of the original one (fitted to the unscrambled Y data), than the risk of chance correlation for the original model is negligible.

External validation of the final model was performed on a validation set of six compounds not used in the generation of the model. The external predictive capability of the model was quantified by the predictive squared correlation coefficients $q_{EXT}{}^2$ and the external standard deviation error of prediction $SDEP_{EXT}$.

The applicability domain of the final model was assessed and visualized by the Williams plot (a scatter plot of the standardized cross-validated residual versus leverages). This graph allows detecting outliers and defines the boundary of the applicability domain. Compounds with standardized residuals greater than three are considered to be outliers, while influential compounds are those with a leverage (h) higher than the critical value h^* ($h^* = 3p'/n$, where p' is the number of predictor variables plus one, and n is the number of training compounds). Predictions for compounds whose leverage values exceed the critical one should be considered unreliable.

Acknowledgments

This work was supported by Croatian Ministry of Science, Education and Sports through Grant No. 178-0982929-2259.

References and notes

1. Komiyama, M.; Takeuchi, T.; Mukawa, T.; Asanuma, H. *Molecular Imprinting: From Fundamentals to Applications*; Wiley: Weinheim, 2003.
2. Turiel, F.; Martin-Esteban, A. *Anal. Bioanal. Chem.* **2004**, *378*, 1876.
3. Haupt, K.; Mosbach, K. *Chem. Rev.* **2000**, *100*, 2495.
4. Ye, L.; Mosbach, K. *Chem. Mater.* **2008**, *20*, 859.
5. Haupt, K. *Chem. Commun.* **2003**, 171.
6. Woodward, A. W.; Bartel, B. *Ann. Bot.* **2005**, *95*, 707.
7. Napier, R. M. *J. Plant Growth Regul.* **2001**, *20*, 244.
8. Dharmasiri, N.; Dharmashiri, S.; Estelle, M. *Nature* **2005**, *435*, 441.
9. Kepinski, S.; Leyser, O. *Nature* **2005**, *435*, 446.
10. Tan, X.; Calderon-Villalobos, L. I. A.; Sharon, M.; Zheng, C.; Robinson, C. V.; Estelle, M.; Zheng, N. *Nature* **2007**, *446*, 640.
11. Woo, E.-J.; Marshall, J.; Bauly, J.; Chen, J.-G.; Venis, M.; Napier, R. M.; Pickersgill, R. W. *EMBO J.* **2002**, *21*, 2877.
12. Kugimiya, A.; Takeuchi, T. *Anal. Chim. Acta* **1999**, *395*, 251.
13. Kugimiya, A.; Takeuchi, T. *Anal. Sci.* **1999**, *15*, 29.
14. Chen, C.; Chen, Y.; Zhou, J.; Wu, C. *Anal. Chim. Acta* **2006**, *569*, 58.
15. Zhang, Y.; Li, Y.; Hu, Y.; Li, G.; Chen, Y. *J. Chromatogr., A* **2010**, *1217*, 7337.
16. Baggiani, C. In *Molecularly Imprinted Materials*; Yan, P., Ramström, O., Eds.; Marcel Dekker: New York, 2005; pp 517–552.
17. Holland, N.; Frisby, J.; Owens, E.; Hughes, H.; Duggan, P.; McLoughlin, P. *Polymer* **2010**, *51*, 1578.
18. Muñoz, M. A.; Guardado, P.; Hidalgo, J.; Carmona, C.; Balón, M. *Tetrahedron* **1992**, *48*, 5901.
19. Carić, D.; Tomišić, V.; Kveder, M.; Galić, N.; Pifat, G.; Magnus, V.; Šoškić, M. *Biophys. Chem.* **2004**, *111*, 247.
20. Šoškić, M.; Magnus, V. *Bioorg. Med. Chem.* **2007**, *15*, 4595.
21. Šoškić, M.; Magnus, V. *QSAR Comb. Sci.* **2009**, *28*, 1276.
22. Baggiani, C.; Giraudi, G.; Giovannoli, C.; Trotta, F.; Vanni, A. *J. Chromatogr., A* **2000**, *883*, 119.
23. Hansch, C.; Leo, A.; Hoekman, D. *Exploring QSAR. Hydrophobic, Electronic and Steric constants*; American Chemical Society: Washington, DC, 1995.
24. *TSAR*, Version 3.3, Oxford Molecular Ltd., 2000.
25. Bio-Loom, Version 1.5, Biobyte Corp., Claremont, USA.
26. Todeschini, R.; Ballabio, D.; Consoni, V.; Mauri, A.; Pavan, M. MobyDigs, Version 1.0, Talete srl, 2004.
27. Draper, N. R.; Smith, H. *Applied Regression Analysis*; Wiley: New York, 1966.
28. Wold, S.; Eriksson, L. In *Chemometric Methods in Molecular Design*; van de Waterbeemd, H., Ed.; VCH: Weinheim, 1995; pp 309–318.
29. Tropscha, A.; Gramatica, P.; Gombar, V. K. *QSAR Comb. Sci.* **2003**, *22*, 69.
30. Gramatica, P. *QSAR Comb. Sci.* **2007**, *26*, 694.